CHAPTER V

EFFECT OF Sr SUBSTITUTED $La_{2-x}Sr_xNiO_{4\pm\delta}$ (x = 0, 0.2, 0.4, 0.6, AND 0.8) ON OXYGEN STOICHIOMETRY AND OXYGEN TRANSPORT PROPERTIES

5.1 Abstract

Stoichiometry, phase and oxygen diffusion properties of $La_{2-x}Sr_xNiO_{4\pm\delta}$ with x = 0.2, 0.4, 0.6, and 0.8 were investigated in this study. The compounds were prepared via a sol-gel method. Iodometric titration and thermogravimetric analysis were used to determine the oxygen non-stoichiometry. Over the entire compositional range the samples exhibited the I4/mmm tetragonal structure and were in the hyperstoichiometric form with the minimum value δ = 0.14 at x = 0.4. Mixed effects between reduction of oxygen excess and increasing valence of Ni were found as charge compensation mechanisms; the former dominated at a low level of substitution, $x \leq 0.4$, while the latter dominated at higher levels of Sr ($0.4 \leq x \leq 0.8$). Oxygen tracer diffusion (D*) and surface exchange coefficients (k*) of the polycrystalline samples were determined by the oxygen isotopic exchange experiment over the temperature range of 550-800°C. Tracer diffusivity was found to follow an increasing trend with increasing oxygen content. Consequently the highest diffusion coefficient was found for the minimum amount of Sr substitution, x = 0.2, continuously decreasing with x until x = 0.6. An unusual increase in D* was observed when the Sr content increased up to x = 0.8. Among the Sr substituted compositions studied, $La_{1.2}Sr_{0.8}NiO_{4\pm\delta}$ was found to exhibit good oxygen diffusivity and a matching thermal expansion coefficient with typical SOFC electrolytes while exhibiting the highest total conductivity.

(**Keywords**: Oxygen content, Oxygen diffusion, Ruddlesden-Popper, Sr substitution on Lanthanum nickelate, SOFCs)

5.2 Introduction

Materials with mixed ionic and electronic conducting properties (MIECs) have attracted much attention for electrochemical applications, such as SOFCs, high temperature steam electrolysis, sensors and ceramic membranes [1-2]. Most studies concerned with these mixed conducting materials especially for the SOFC cathodes, have focused on perovskite-type oxides such as lanthanum manganite, lanthanum cobaltite and lanthanum nickelate [3-4]. With SOFC development directed towards operation in the intermediate temperature range (400-600°C), these materials do not satisfy all of the technological requirements especially, mechanical compatibility with other cell components and conductivity [3]. Materials with the Ruddlesden-Popper type structure, A_2BO_4, have attracted much interest recently due to their mixed conducting properties while maintaining high electrical conductivity in the targeted temperature range [5-8].

$La_2NiO_{4+\delta}$ and related materials have been proposed as candidates for energy related electrochemical applications because of their excellent transport and electrocatalytic properties [2,7-10]. Moreover, materials in this group also exhibit coefficient of thermal expansion (CTE) values in the range of $12.4\text{-}13.6\times10^{-6}$ K^{-1}, close to the common SOFC electrolyte materials such as the ceria-based electrolytes (13.2×10^{-6} K^{-1}) [4,11]. The $La_2NiO_{4+\delta}$ structure is made up of sheets of (NiO_6) corner sharing octahedra, interleaved with La_2O_2 layers in which the additional oxygen could be localized. The compound is therefore able to accept oxygen overstoichiometry that leads to potentially high oxygen diffusivity compared to that of the common cathode materials [1-2,7,9,12]. However, due to insufficient electrical conductivity, 10-70 S/cm [8], in $La_2NiO_{4+\delta}$, attempts to improve such properties which have been conducted through substitution of the A site with alkaline-earth ions. Ca and Sr are the most popular dopants due to their compatible ionic radii. However, Ca has been found to have little effect on electrical conductivity, while the replacement of La by Sr leads to a much larger improvement [5-6,10,13].

Most efforts on $La_{2-x}Sr_xNiO_4$ (LSNO) have been devoted to understanding structural stability, electrical and thermal behavior of $La_{2-x}Sr_xNiO_{4+\delta}$ compounds with only a few investigations of the transport of conducting species in the system

[5-6,8,11,13-16]. Zhao *et al.* studied the lanthanum deficient compound, $La_{2-x}NiO_{4+\delta}$ (x = 0, 0.05) [17]. They found that the D* and k* values for $La_{1.95}NiO_{4.13}$ were higher than that of the stoichiometric compound. Kharton *et al.* studied factors affecting ionic transport in oxygen-hyperstoichiometric phases of A_2BO_4 structures such as the lanthanum nickelates and cuprates. They found that decreasing radii of the rare-earth cations in the A-sublattice of both cuprates and nickelates led to a dramatic decrease in ionic transport, similar to that observed with perovskite oxides [18]. Skinner and Kilner studied oxygen transport of $La_{2-x}Sr_xNiO_{4+\delta}$ (x = 0, 0.1) and found that oxygen diffusivity of $La_{1.9}Sr_{0.1}NiO_{4+\delta}$ was higher than that of $La_xSr_{1-x}Co_yFe_{1-y}O_{3-\delta}$, particularly at lower temperatures, but lower than that of $LaCoO_3$. However, $La_{1.9}Sr_{0.1}NiO_{4+\delta}$ appears to be more stable than either of these two materials in terms of thermal expansion behavior at high temperatures [19]. There are still very few reports on the ionic transport in Sr substituted $La_2NiO_{4+\delta}$, particularly with higher Sr substitution content.

In this work, we aim to extend the knowledge of oxygen transport in LSNO to a higher level of Sr substitution. Effects of Sr substitution in $La_{2-x}Sr_xNiO_{4+\delta}$ (x = 0.2, 0.4, 0.6, and 0.8) on the oxygen stoichiometry, phase and transport properties were investigated in this research.

5.3 Experimental

5.3.1 Preparation of $La_{2-x}Sr_xNiO_{4+\delta}$ (x = 0.2, 0.4, 0.6, and 0.8)

$La_{2-x}Sr_xNiO_{4+\delta}$ (x = 0.2, 0.4, 0.6, and 0.8) powders were prepared by a sol-gel method following the process described in our previous work [11]. Lanthanum (III) acetate hydrate ($(CH_3COO)_3La{\bullet}xH_2O$, 99.9%, Sigma-Aldrich), strontium acetate ($(CH_3COO)_2Sr$, 99.995%, Sigma-Aldrich), and nickel acetate ($(CH_3COO)_2Ni{\bullet}4H_2O$, 98%, Sigma-Aldrich) were dissolved in deionized water. The mixture was homogeneously stirred to obtain a clear solution before adding ethanolamine (Labscan Co.), which was used as the directing agent. The mixture was stirred continuously for 6 h before being left at room temperature to gel. The gel was

then calcined at 1050°C with a heating rate of 3°C/min for 2 h, resulting in black powders.

To obtain high density samples for $^{18}O_2$ isotope exchange measurements, the synthesized powders were ground, uniaxially pressed at 65 MPa followed by isostatically pressing at 300 MPa to form 13 mm diameter pellets. The pellets were fired in a box furnace at 1400°C for 5 hr with a heating rate of 5°C/min in air. The Archimedes' method was used to measure the density of the sintered samples to ensure that the samples were adequately dense for the diffusion analysis. All samples tested achieved a density greater than 95% of the theoretical density for the material, ensuring only closed porosity was present in the samples.

5.3.2 Oxygen Content

Oxygen content in the $La_{2-x}Sr_xNiO_{4+\delta}$ samples was determined using two methods. The first one is an indirect measurement through a reduction of Ni^{3+}/Ni^{2+} ions to Ni using iodometric titration. The other is the determination of the amount of oxygen via sample weight loss under a reducing atmosphere through thermogravimetric analysis (TGA).

For the analysis using the first method, oxygen overstoichiometry (δ) of the compound was assumed to be directly correlated to the Ni^{3+} content according to the formulation $La_{2-x}Sr_xNi^{2+}_{1-\tau}Ni^{3+}_{\tau}O_{4+\tau/2}$ with $\delta = \tau/2$ [1, 20]. Ni^{3+} content (τ) was determined by iodometry. In the experiment, 0.1 g of sample was dissolved in a 4 ml HCl solution (ACS, 36.5–38.0%, Alfa Aesar) containing 1 g excess potassium iodide (KI, 99.99%, Alfa Aesar). The experiment was performed under flowing nitrogen to prevent oxidation of Ni ions in air. I^- anions reduce Ni^{3+} to Ni^{2+} forming I_2 (Eq.1). The resulting I_2 was then titrated by sodium thiosulfate solution ($Na_2S_2O_3$, 99.99%, Sigma–Aldrich) using a starch solution (ACS, 1% solution, Alfa Aesar) as the indicator (Eq.2). All reactions are summarized in Eq.3.

$$2Ni^{3+} + 2I^- \rightarrow 2Ni^{2+} + I_2 \quad (1)$$

$$I_2 + 2S_2O_3^{2-} \rightarrow 2I^- + S_4O_62^- \quad (2)$$

Summary: $$2Ni^{3+} + 2S_2O_3^{2-} \rightarrow 2Ni^{2-} + S_4O_6^{2-} \quad (3)$$

To confirm the concentration of $Na_2S_2O_3$, 0.01 M of KIO_3 (99.995%, Sigma–Aldrich) in 0.01 M of KI and 1 M of H_2SO_4 (ACS, 95.0-98.0%, Alfa Aesar) was titrated by $Na_2S_2O_3$ solution using starch as the indicator as shown in Eq.4 [20]. Knowing the amount of the reducing agent used, oxygen overstoichiometry, δ, could then be calculated.

$$6S_2O_3^{2-} + IO_3^- + 6H^+ \rightarrow I^- + 3S_4O_6^{2-} + 3H_2O \quad (4)$$

To confirm the result from the iodometry, thermogravimetric analysis (TGA) was performed. The TGA (TGA/STDA851e Mettler Toledo) experiment was done under a reducing atmosphere using 5% H_2/Ar flowing gas (BIG, Thailand). The analysis was performed from room temperature up to 1000°C with a heating rate of 5°C/min. The $La_{2-x}Sr_xNiO_{4+\delta}$ compound was reduced to $La_{2-x}Sr_xNiO_4$ in the first stage of the test (Eq.5). Further exposure to the reducing atmosphere at higher temperatures should result in the decomposition of the multi–cation compounds into La_2O_3, SrO and Ni metal (Eq. 6). The total reaction involved is shown in Eq. 7 in which the amount of oxygen in the starting material could be calculated, and the overstoichiometric amount of oxygen, δ, could then be determined.

$$La_{2-x}Sr_xNiO_{4+\delta} + \delta H_2 \rightarrow La_{2-x}Sr_xNiO_4 + \delta H_2O \quad (5)$$

$$La_{2-x}Sr_xNiO_4 + (1+0.5x)H_2 \rightarrow (1-0.5x)La_2O_3 + xSrO + Ni + (1+0.5x) + \delta H_2O \quad (6)$$

$$La_{2-x}Sr_xNiO_{4+} + \{(1+0.5x)+\delta\}H_2 \rightarrow (1-0.5x)La_2O_3 + xSrO + Ni + \{(1+0.5x)+\delta\}H_2O \quad (7)$$

5.3.3 Oxygen Diffusion and Surface Exchange Coefficients

Isotopic oxygen transport and surface exchange coefficients were investigated for the $La_{2-x}Sr_xNiO_{4+\delta}$ (x = 0.2, 0.4, 0.6, and 0.8) pellets. The sintered pellets were ground with SiC paper (1000 and 800 grit), and were then polished with successive grades of diamond suspension of 15, 6, 3, 1 and 0.25 μm. Oxygen isotopic exchange was performed over the temperature range of 550 to 800°C at a nominal pressure of 200 mbar. The polished samples were annealed at the testing temperature in research grade $^{16}O_2$ (> 99.9995%, BOC, UK) for a period of at least

ten times the exchange time with $^{18}O_2$ (97.1%, Isotec Inc., USA) to ensure that an equilibrium was established. ^{18}O exchange was performed immediately after the equilibration step with the exchange times between 45 and 240 mins, depending on the exchange temperature. All samples were immediately quenched to room temperature after the ion exchange experiment.

After removing the sample from the exchange tube, the pellets were sectioned using a diamond bladed saw perpendicular to the exchanged surface. The exposed cross-sections were again polished using diamond suspensions, as described above and mounted together (top surfaces in contact) to perform the Secondary Ion Mass Spectrometry (SIMS) analysis. All the exchanged samples were measured by time-of-fight SIMS (ToF–SIMS) on a ToF-SIMS5 machine (ION–TOF GmbH, Münster, Germany) equipped with a bismuth LMIG pulsed gun incident at 45°. A 25 kV Bi^+ primary ion beam was used to generate the secondary ions using burst alignment mode (eight pulses) for analysis and a Cs^+ beam (2 kV) incident at 45° for sputtering. The distribution of the oxygen isotopes (^{18}O and ^{16}O) as well as other characteristic relevant secondary ion species (e.g. LaO^-, NiO^-, and SrO^-) in $La_{2-x}Sr_xNiO_{4+\delta}$ samples with x = 0.2 at 625–800°C and at x = 0.8 were measured using SIMS imaging mode (image acquisition interspersed with Cs^+ sputtering of the surface). However, for the samples with low isotope concentration, $La_{2-x}Sr_xNiO_{4+\delta}$ samples with x = 0.2 (at 500°C), x = 0.4 and x = 0.6, the secondary ions (^{18}O, ^{16}O LaO^-, NiO^-, and SrO^-) from the samples were measured in the depth profiling mode. Oxygen diffusion profiles were obtained by summing all of the ^{16}O (^{18}O) images together and summing all the columns (or rows) of this image, to obtain a ^{16}O (^{18}O) linescan. Subsequently the number of counts was normalized to obtain the ^{18}O fraction corrected for the background isotope fraction and the isotope fraction of the annealing gas, as described by De Souza *et al.* [21]. Tracer diffusion coefficients, D*, and surface exchange coefficients, k*, of each $La_{2-x}Sr_xNiO_{4+\delta}$ composition were determined by fitting the diffusion data to the solution of the diffusion equation for diffusion in a semi-infinite medium with surface limitation as given by Crank, and described in [21].

Phase analysis was performed on all samples. The samples were analyzed using a Philips PW 1700 Series x-ray diffractometer with Cu Kα source (λ = 1.5418 Å) over 20-80° 2θ range. Full profile fitting and refinement was performed to confirm the crystal structure along with the corresponding lattice parameters using JADE 9 X-ray analysis software (MDI, CA, USA).

5.4 Results and Discussion

5.4.1 Oxygen Content

Table 5.1 shows the amount of oxygen over stoichiometry (δ) and the corresponding valence of Ni of the $La_{2-x}Sr_xNiO_{4-\delta}$ samples obtained from the iodometry and TGA. The δ values calculated from both methods are in good agreement, and are within 15% of each other. With the results from iodometry and TGA in good agreement and in order for the data to be easily discussed, the oxygen non-stoichiometry values referred to in the discussion section are the values obtained from the titration analysis.

With Sr substitution onto the La site at x = 0.2, the oxygen content was found to equal to δ = 0.14. This value is significantly lower than what has been previously reported in the literature by Skinner and Kilner for x = 0, where the oxygen excess content was found to be 0.24 [19]. The corresponding valence of Ni was found to +2.48 at x = 0.2. This result indicates that the compensation of the Sr^{2+} cation substitution onto the La^{3+} site was mainly accommodated by the reduction of the excess O^{2-} with a small compensation from the change of Ni valence. A similar result was also reported by Skinner and Kilner who studied samples with 5% Sr substitution for La in $La_{2-x}Sr_xNiO_{4+\delta}$. They observed a decrease in δ from 0.24 to 0.19 upon the Sr substitution while Ni valence stayed constant at +2.48 in both cases [19].

With a higher level of Sr substitution, x = 0.4 and 0.6, the δ values were found to change slightly from 0.14 to 0.15 and 0.17, while the average Ni valence was found to increase continuously, from +2.48 to +2.70 and +2.94 for x = 0.2, 0.4 and 0.6, respectively. Such results show that under the conditions used in this

work, $La_{2-x}Sr_xNiO_{4\pm\delta}$ always exists as compounds with oxygen hyperstoichiometry with the minimum δ value of approximately 0.14. This differs from the results found by many authors who have reported a constant decrease in the amount of oxygen with increasing Sr substitution [13,22-26]. The majority of reports proposed the reason for the continuously decreasing oxygen content, as being associated with moving from the reduction in the number of oxygen interstitials to oxygen vacancy formation upon higher Sr substitution, with structural instability of the perovskite units if a large amount of Ni^{3+} were to be formed [25]. Aguadero *et al.* reported the critical composition to be $La_{1.5}Sr_{0.5}NiO_4$ where the average Ni valence cannot exceed +2.5; therefore with higher Sr substitution, the compound becomes oxygen deficient [13]. The discrepancy in the results likely arises from how the compounds were synthesized along with slight differences in the experimental details.

With a higher amount of Sr substituted for La, at $x = 0.8$, a slight increase in δ was found while a significant increase in Ni oxidation state was observed. The δ value was determined to be 0.23, and the corresponding Ni valence corresponded to +3.26. The higher than 3 average valence of Ni indicates that Ni^{4+} was formed for the $x = 0.8$ composition. Although the +4 oxidation state of Ni is rarely found in $La_{2-x}Sr_xNiO_{4+\delta}$ compounds, this situation has been reported previously by Makhnach *et al.* in Sr-rich $La_{2-x}Sr_xNiO_{4+\delta}$ ($x = 1$ or 1.4) when the synthesis conditions were under high temperature and oxygen partial pressure [14].

5.4.2 X-Ray Diffraction Analysis

Fig. 5.1 shows XRD patterns of the sintered $La_{2-x}Sr_xNiO_{4+\delta}$ samples used in the oxygen exchange experiment. Over the whole range of compositions tested, the samples exhibit the Ruddlesden-Popper (A_2BO_4) structure, with the I4/mmm tetragonal crystal structure, in agreement with what has been reported by others [13-14,19,23]. Minor quantities of NiO were found as impurities when $x = 0.4$, which may slightly affect the δ value measured. The δ value in $La_{2-x}Sr_xNiO_{4+\delta}$ for samples with such impurity is expected to be slightly lower than the calculated one due to the lower probability of Ni being in the Ni^{3+} state in the NiO than that in $La_{2-x}Sr_xNiO_{4+\delta}$. At the highest level of Sr substitution, $x = 0.8$, however, additional peaks besides I4/mmm were observed. These peaks arise from the lower symmetry

structure and could be identified as the orthorhombic structure adopting space group Fmmm.

Unit cell parameters and the unit cell volume of the Sr substituted samples were calculated and are shown in Fig. 5.2. On increasing the amount of Sr substitution from x = 0.2 to x = 0.4, the a lattice parameter decreased while the c parameter increased. Such changes in the lattice parameters can be explained by the change in the amount of oxygen excess and the average Ni valence reported in the previous section. With an increase of Sr substitution from x = 0.2 to 0.4, a slight increase in the amount of oxygen excess could be observed. However, a much more significant increase in the Ni^{3+} content was found. The higher oxidation state of Ni (Ni^{2+} to Ni^{3+}) resulted in a decrease in Ni–O bond length and thus a decreasing lattice parameter in the perovskite unit, and therefore, a decreasing lattice parameter in the a, b direction. The slight increase in the c parameter could be explained by the replacement of La^{3+} by Sr^{2+}(1.27 Å) which has larger ionic radius than La^{3+}(1.20 Å) [15]. Both effects resulted in a decrease in total cell volume which is consistent with what has been observed by many others for x = 0 to 0.5 [5,13,15-16].

At x = 0.6, an opposite trend was observed. The a parameter was found to slightly increase and the c parameter was found to decrease. Such changes were also observed in other works when a large amount of Sr was substituted for La in the $La_{2-x}Sr_xNiO_{4\pm\delta}$ compound and could be explained by Jahn-Teller distortion [5, 13, 15]. However, with x = 0.8, the a parameter did not increase; it decreased instead while the c parameter continued to decrease. This is likely caused by the oxidation of Ni^{3+} to Ni^{4+}. While the substitution of Sr^{2+} for La^{3+} induces an increase in (La,Sr)–O bond length that could lead to an increase in the c lattice parameter, the change of oxidation state from lower to higher charge i.e. Ni^{3+} to Ni^{4+} could result in a significant decrease in Ni–O bond length [5]. Both effects compete with each other, and in this case, the decrease in Ni–O bond length dominates leading to an overall decrease in the c parameter observed.

5.4.3 Oxygen Diffusion and Surface Exchange Coefficients

Oxygen isotopic exchange and SIMS analyses were performed on the sintered specimens. Elemental LaO^-, NiO^-, and SrO^- mapping results showed homogeneous distribution of all species for all samples, except for x = 0.4 in which

areas with higher NiO^- counts were observed. This result is consistent with the XRD analysis of the $x = 0.4$ composition where small amounts of NiO were observed (Fig. 5.1).

Table 5.2 shows the effect of Sr substitution on the oxygen diffusion coefficients (D*) and surface exchange coefficients, k*, at 800°C. A relatively small change in the surface exchange coefficient was observed across the compositional range studied. This is consistent with previous reports where the surface exchange was found to be more sensitive to parameters influencing the surface state such as synthesis method, and orientation of the crystal [20, 27]. The oxygen diffusion coefficients, however, were found to be very sensitive to the amount of Sr substitution. Examples of SIMS image and oxygen diffusion profile of $La_{1.8}Sr_{0.2}NiO_{4+\delta}$ recorded at 800°C are shown in Fig. 5.3.

By substituting a small amount of La^{3+} with Sr^{2+}, i.e. $x = 0.2$, D* decreased approximately by one order of magnitude with Sr substitution. This trend has previously been observed by other authors [6,9,18-19,21]. For example, Skinner and Kilner found that the oxygen diffusion coefficient for 5% Sr substituted $La_{2-x}Sr_xNiO_4$ was lower than in the material with no substitution [19]. Such reduction in the D* value could be explained by a decrease in the amount of oxygen interstitials in the compounds in which δ was reduced.

The $La_{1.8}Sr_{0.2}NiO_{4+\delta}$ compound was further evaluated to understand changes in activation energy of the ionic transport in the system compared to that with no substitution and with 5% Sr substitution [19]. Additional oxygen exchange experiments were performed for this composition at temperatures between 550-800°C. The obtained tracer diffusion coefficients and surface exchange coefficients of the $La_{1.8}Sr_{0.2}NiO_{4+\delta}$ compound at these temperatures are shown in Fig. 5.4a and Fig. 5.4b, respectively. As expected, D* follows the Arrhenius law, increasing with increasing temperature. Since the diffusivity depends on the mobility of oxygen atoms, which is strongly affected by temperature, with decreasing temperature the mobility of oxygen ions also decreases. The activation energy for D* was found to be 0.60 eV (Table 5.3) close to the values reported by Skinner and Kilner ($E_a = 0.57$ eV) for $La_{1.8}Sr_{0.2}NiO_{4+\delta}$ [19] and lower than that with no Sr substitution ($E_a = 0.85$ eV).

The surface exchange coefficients, k*, for $La_{1.8}Sr_{0.2}NiO_{4+\delta}$ were found to also follow the Arrhenius-type behaviour for the low temperature range (550-700°C) with the values similar to those found in the literature for x = 0 and x = 0.2 [19, 22]. However, the k* value do not follow the same trend at 800°C. The reason for such deviation is not yet conclusive and requires further investigation.

At 800°C for higher levels of Sr substitution, x = 0.4 to 0.6 the diffusivity values decrease by several orders of magnitude as shown in Fig. 4(a) and Table 5.2. At x = 0.2, D* was found to be 1×10^{-9} cm^2s^{-1}, while it was found that D* was 1×10^{-12} cm^2s^{-1} for x = 0.4 and 3×10^{-13} cm^2s^{-1} for x = 0.6. Considering the amount of oxygen excess in the compound which rarely changed between x = 0.2 to 0.6, the decrease in D* is unlikely to be due to the concentration of the conducting species alone but the change in mobility of the conducting species (oxygen ion).

With higher Sr substitution (x > 0.6), a dramatic increase of approximately 4 orders of magnitude in D* was observed, from 3×10^{-13} cm^2s^{-1} for x = 0.6 to 2×10^{-9} cm^2s^{-1}, for x = 0.8. Such a large increase in the diffusion coefficient is likely due to a significant increase in excess oxygen content (δ) which is almost as high as that of the undoped compound (Table 5.1). However, it is worth noting that the D* value is almost two orders of magnitude lower than that of the undoped composition even with similar oxygen hyperstoichiometric amount. The much lower diffusivity for x = 0.8 is likely due to lower mobility of oxygen ion in the Sr substituted compound compared to that with no Sr substitution. From our previous work, this composition also exhibits the highest electrical conductivity and lowest thermal expansion coefficient over the range of composition studied (x = 0-0.8) [11]. Although, D* and k* of $La_{1.2}Sr_{0.8}NiO_{4\pm\delta}$ are lower than the values of one of the most promising cathode candidates for IT-SOFCs, $La_{1-x}Sr_xCo_{1-y}Fe_yO_{3-\delta}$ (LSCF) perovskite (D* ~ 3×10^{-8} cm^2s^{-1} and k* ~ 2×10^{-7} cm s^{-1}) [19], the compound exhibits other superior properties. It has higher electrical conductivity at intermediate temperature, as high as 160 Scm^{-1} at 500°C, and low thermal expansion coefficient much closer to common IT-SOFC electrolytes, 12.4×10^{-6} $°C^{-1}$ (400-700°C) have been previously reported [11].

5.5 Conclusions

$La_{2-x}Sr_xNiO_{4+\delta}$ (x = 0.2, 0.4, 0.6, and 0.8) synthesized via a sol-gel method exhibited the I4/mmm tetragonal structure with a trace amount of Fmmm orthorhombic phase for x = 0.8 and traces of NiO for x = 0.4. Over the entire range of the compositions tested, the samples exhibited oxygen hyperstoichiometry with the minimum δ = 0.14 for x = 0.4. At low levels of Sr substitution ($x \leq 0.2$), the lower valence substitution on the A-site was accommodated by decreasing the oxygen interstitial content. At higher substitution levels, $0.4 < x < 0.6$, the accommodation of Ni with higher valence e.g. Ni^{3+} to maintain charge neutrality became increasingly important. At x = 0.8, the charge compensation was attributed almost entirely to an increase in Ni oxidation state where the average Ni valence was found to be +3.26. D* was found to be very sensitive to the doping amount while k* changed very little with the amount of doping. At 800°C, D* decreased with the increasing amount of Sr from 1×10^{-9} cm^2s^{-1} at x = 0.2 and reached the minimum value of 3×10^{-13} cm^2s^{-1} at x = 0.6, then increasing again to 2×10^{-9} cm^2s^{-1} at x = 0.8. The decreasing D* seems to follow the amount of oxygen excess in the compounds up until x = 0.4, then other mechanisms apparently take over.

5.6 Acknowledgements

This work was partially funded by the postgraduate education and research programs in Petroleum and Petrochemical Technology (PPT Consortium), Rachadapisake Sompote fund, Chulalongkorn University, the Development and Promotion of Science and Technology, Thailand project (DPST), and the National Metal and Materials Technology Center (MTEC), Thailand for financial support. I would like to thank Dr. Sumittra Charojrochkul from MTEC, Thailand and staff at the Department of Materials, Imperial College London. This research was also supported by a Marie Curie Intra European Fellowship within the seventh European Community Framework Programme (PIEF-GA-2009-252711) and from King Abdullah University of Science & Technology, Saudi Arabia (for M.B).

5.7 References

[1] Boehm, E., Bassat, J.-M., Steil, M.C., Dordor, P., Mauvy, F., and Grenier, J.-C. (2003) Oxygen transport properties of $La_2Ni_{1-x}Cu_xO_{4+\delta}$ mixed conducting oxides. Solid State Sci., 5, 973-981.

[2] Routbort, J.L., Doshi, R., and Krumpelt, M. (1996) Oxygen tracer diffusion in $La_{1-x}Sr_xCoO_3$. Solid State Ionics, 90, 21-27.

[3] Chiba, R., Yoshimura, F., and Sakurai, Y. (1999) An investigation of $LaNi_{1-x}Fe_xO_3$ as a cathode material for solid oxide fuel cells. Solid State Ionics, 124, 281-288.

[4] Ullmann, H., Trofimenko, N., Tietz, F., Stöver, D., and Ahmad-Khanlou, A. (2000) Correlation between thermal expansion and oxide ion transport in mixed conducting perovskite-type oxides for SOFC cathodes. Solid State Ionics, 138, 79-90.

[5] Tang, J.P., Dass, R.I., and Manthiram, A. (2000) Comparison of the crystal chemistry and electrical properties of $La_{2-x}A_xNiO_4$ (A = Ca, Sr. and Ba). Mater. Res. Bull., 35, 411-424.

[6] Hui, Z., Qiang, L., and LiPing, S. (2011) Ln_2MO_4 cathode materials for solid oxide fuel cells. Sci. China Chem., 54, 898-910.

[7] Greenblatt, M. (1997) Ruddlesden–Popper $Ln_{n+1}Ni_nO_{3n+1}$ nickelates: Structure and properties. Solid State & Mater. Sci., 2, 174-183.

[8] Vashook, V.V., Yushkevich, I.I., Kokhanovsky, L.V., Makhnach, L.V., Tolochko, S.P., Kononyuk, I.F., Ullmann, H., and Altenburg, H. (1999) Composition and conductivity of some nickelates. Solid State Ionics, 119, 23-30.

[9] Amow, G. and Skinner, S. J. (2006) Recent developments in Ruddlesden-Popper nickelate systems for solid oxide fuel cell cathodes. J. Solid State Electrochem., 10, 538-46.

[10] Fontaine, M. L., Laberty-Robert, C., Ansart, F., and Tailhades, P. (2006) Composition and porosity graded $La_{2-x}NiO_{4+\delta}$ ($x \geq 0$) interlayers for SOFC: control of the microstructure via a sol-gel process. J. Power Source, 156, 33-38.

[11] Inprasit, T., Limthongkul, P., and Wongkasemjit, S. (2010) Sol-gel and solid-state synthesis and property study of $La_{2-x}Sr_xNiO_4$ ($x \leq 0.8$). J. Electrochem. Soc., 157, B1726-B1730.

[12] Darcovich, K., Whitfield, P.S., Amow, G., Shinagawa, K., and Miyahara, R.Y. (2005) A microstructure based numerical simulation of microwave sintering of specialized SOFC materials. J. Eur. Ceram. Soc., 25, 2235-2240.

[13] Aguadero, A., Escudero, M. J., Perez, M., Alonso, J. A., Pomjakushin, V., and Daza, L. (2006) Effect of Sr content on the crystal structure and electrical properties of the system $La_{2-x}Sr_xNiO_{4+\delta}$ ($0 \leq x \leq 1$). Dalton Trans., 4377-4383.

[14] Makhnach, L.V., Pankov, V.V., and Strobel, P. (2008) High–temperature oxygen non-stoichiometry, conductivity and structure in strontium-rich nickelates $La_{2-x}Sr_xNiO_{4-\delta}$ ($x = 1$ and 1.4). Mater. Chem. Phys., 111, 125-130.

[15] Gopalakrishnan, J., Colsmann, G., and Reuter, B. (1977) Studies on the $La_{2-x}Sr_xNiO_4$ ($0 \leq x \leq 1$) system. J. Solid State Chem., 22, 145-149.

[16] Takada, Y., Kanno, R., Sakano, M., and Yamamoto, O. (1990) Crystal chemistry and physical properties of $La_{2-x}Sr_xNiO_3$ ($0 \leq x \leq 1.6$). Mater. Res. Bull., 25, 293-306.

[17] Zhao, H., Mauvy, F., Lalanne, C., Bassat, J.-M., Fourcade, S., and Grenier, J.-C. (2008) New cathode materials for ITSOFC: Phase stability, oxygen exchange and cathode properties of $La_{2-x}NiO_{4+\delta}$. Solid State Ionics, 179 (35-36), 2000-2005.

[18] Kharton, V.V., Viskup, A.P., Kovalevsky, A.V., Naumovich, E.N., and Marques, F.M.B. (2001) Ionic transport in oxygen–hyperstoichiometric phases with K_2NiF_4-type structure. Solid State Ionics, 143, 337-353.

[19] Skinner, S.J. and Kilner, J.A. (2000) Oxygen diffusion and surface exchange in $La_{2-x}Sr_xNiO_{4+\delta}$. Solid State Ionics, 135, 709-712.

[20] Boehm, E., Bassat, J.M., Dordor, P., Mauvy, F., Grenier, J.C., and Stevens, Ph. (2005) Oxygen diffusion and transport properties in non-stoichiometric $Ln_{2-x}NiO_{4+\delta}$ oxides. Solid State Ionics, 176, 2717-2725.

[21] De Souza, R.A., Zehnpfenning, J., Martin, M., and Maier, J. (2005) Determining oxygen isotope profiles in oxides with Time–of–Flight SIMS. Solid State Ionics, 176, 1465-1471.

[22] Sayers, R., De Souza, R.A., Kilner, J.A. and Skinner, S.J. (2010) Low temperature diffusion and oxygen stoichiometry in lanthanum nickelate. Solid State Ionics, 181, 386-391.

[23] Aguadero, A., Alonso, J.A., Martinez-Lope, M.J., Fernandez-Diaz, M. T., Escudero, M.J., and Daza, L. (2006) In situ high temperature neutron powder diffraction study of oxygen–rich $La_2NiO_{4+\delta}$ in air: Correlation with the electrical behaviour. J. Mater. Chem., 16, 3402-3408.

[24] Junjiang, Z. and Thomas, A. (2009) Perovskite–type mixed oxides as catalytic material for NO removal. Appl. Catal., B, 92, 225-233.

[25] Junjiang, Z., Xiangguang, Y., Xuelian, X., and Keme, W. (2007) Effect of strontium substitution on the activity of $La_{2-x}Sr_xNiO_4$ (x = 0.0—1.2) in NO decomposition. Sci. China, Ser. B, 50, 41-46.

[26] Manthiram, A., Tang, J.P., and Manivannan, V. (1999) Factors influencing the stabilization of Ni^+ in perovskite-related Oxides. J. Solid State Chem., 148(2), 499-507.

[27] Bassat, J.M., Odier, P., Villesuzanne, A., Marin, C., and Pouchard, M. (2004) Anisotropic ionic transport properties in $La_2NiO_{4+\delta}$ single crystals. Solid State Ionics, 167(3-4), 341-347.

Table 5.1 Hyperstoichiometric oxygen content (δ) and the corresponding valence of Ni of $La_{2-x}Sr_xNiO_{4+\delta}$ samples

x, Sr content	δ		Average Valence of Ni	
	Iodometry	**TGA**	**Iodometry**	**TGA**
0	-	0.24[19]	-	+2.48[19]
0.2	0.14 ± 0.03	0.16	+2.48	+2.52
0.4	0.15 ± 0.01	0.14	+2.70	+2.68
0.6	0.17 ± 0.01	0.18	+2.94	+2.96
0.8	0.20 ± 0.02	0.23	+3.20	+3.26

Table 5.2 Tracer diffusion (D*) and surface exchange coefficients (k*) for $La_{2-x}Sr_xNiO_{4+\delta}$

Temp (°C)		Sr content, x, in $La_{2-x}Sr_xNiO_{4+\delta}$ (mol ratio)					
		0[19]	**0.1**[19]	**0.2**	**0.4**	**0.6**	**0.8**
550	D*(cm^2/s)	-	-	1.52×10^{-10}	-	-	-
	k* (cm/s)	-	-	1.18×10^{-8}	-	-	-
625	D*(cm^2/s)	-	-	2.96×10^{-10}	-	-	-
	k* (cm/s)	-	-	3.32×10^{-8}	-	-	-
700	D*(cm^2/s)	3.38×10^{-8}	1×10^{-8}	6.06×10^{-10}	-	-	-
	k* (cm/s)	1.75×10^{-7}	1.74×10^{-7}	1.22×10^{-7}	-	-	-
800	D*(cm^2/s)	1.71×10^{-7}	1.33×10^{-8}	1.06×10^{-9}	1.15×10^{-12}	3.02×10^{-13}	2.26×10^{-9}
	k* (cm/s)	2.55×10^{-6}	6.46×10^{-7}	2.68×10^{-8}	5.47×10^{-8}	2.75×10^{-8}	7.52×10^{-8}

Table 5.3 Activation energy of the diffusion (D*) and surface exchange coefficients (k*) for $La_{2-x}Sr_xNiO_{4+\delta}$

	Activation energy (eV)		
$La_{2-x}Sr_xNiO_{4+\delta}$	**x = 0[19]**	**x = 0.1[19]**	**x = 0.2**
D*	0.85	0.57	0.60
k*	1.61	1.29	1.06

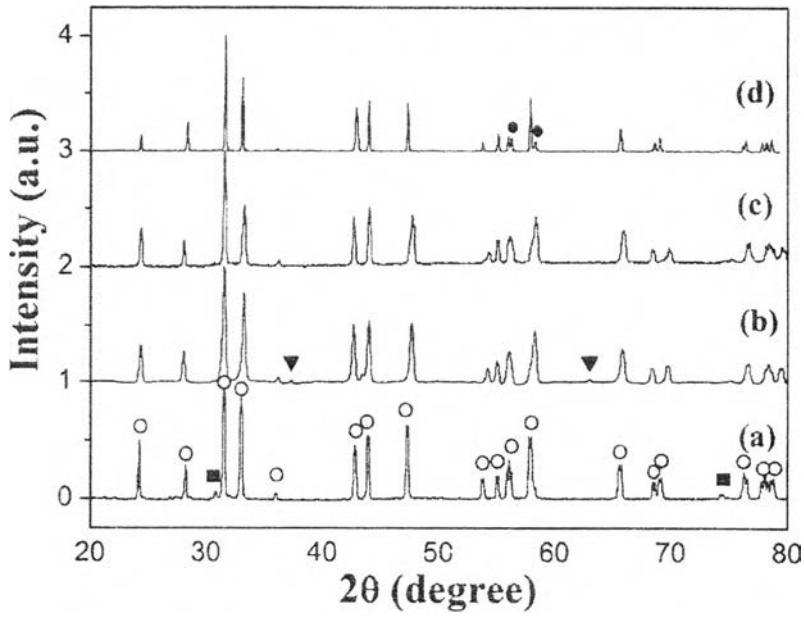

Figure 5.1 XRD pattern of $La_{2-x}Sr_xNiO_{4+\delta}$ sintered pellets before ^{18}O exchange , (a) x = 0.2 ,(b) x = 0.4, (c) x = 0.6 and (d) x = 0.8 (o Tetragonal (I4/mmm), • orthorhom -bic (Fmmm) and ▼ NiO).

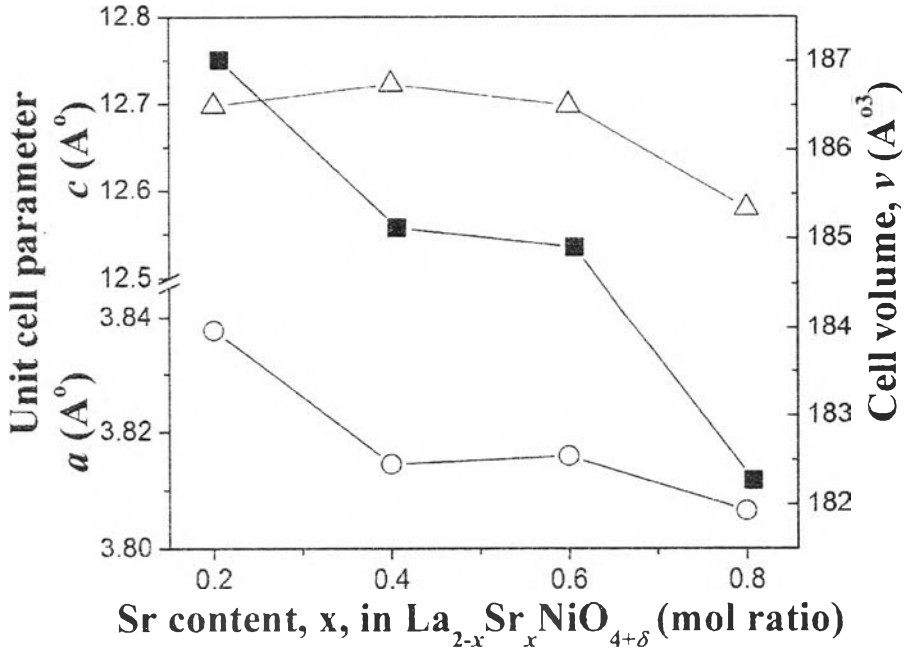

Figure 5.2 Unit cell parameters of $La_{2-x}Sr_xNiO_{4\pm\delta}$: (○) a parameter, (△) c parameter and (■) cell volume.

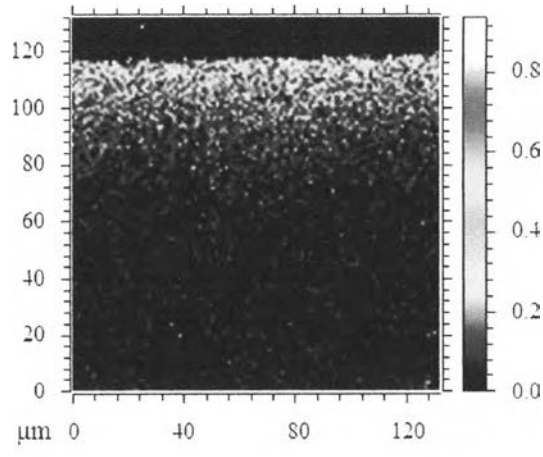

(a)

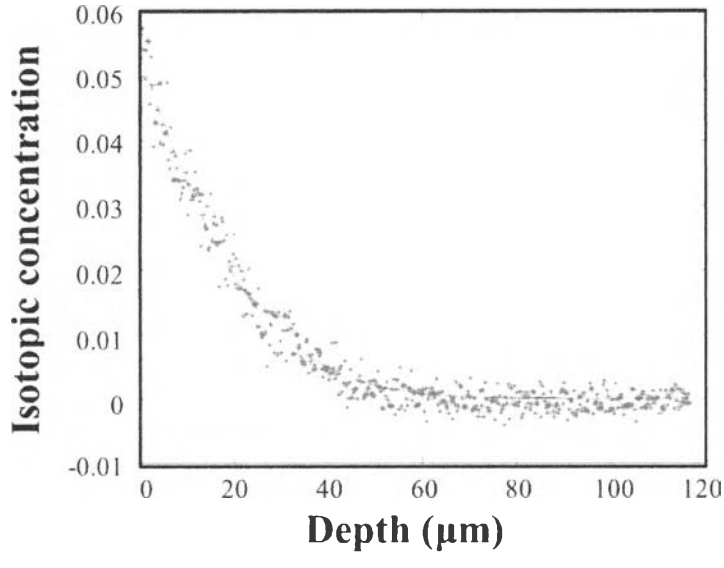

(b)

Figure 5.3 The (a) normalised ^{18}O SIMS image and (b) ^{18}O concentration of $La_{1.8}Sr_{0.2}NiO_{4-\delta}$ after $^{18}O_2$ exchange at 800°C for 2 h.

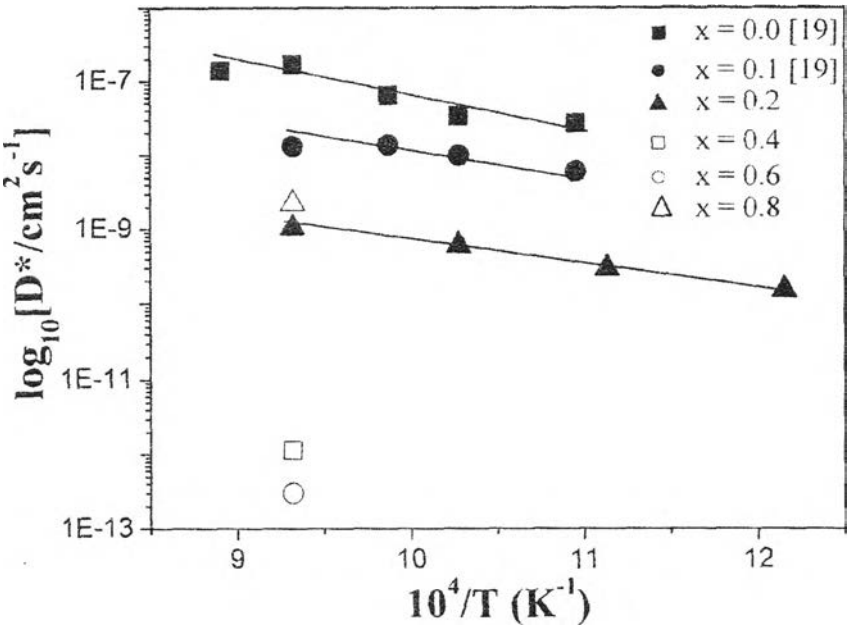

(a)

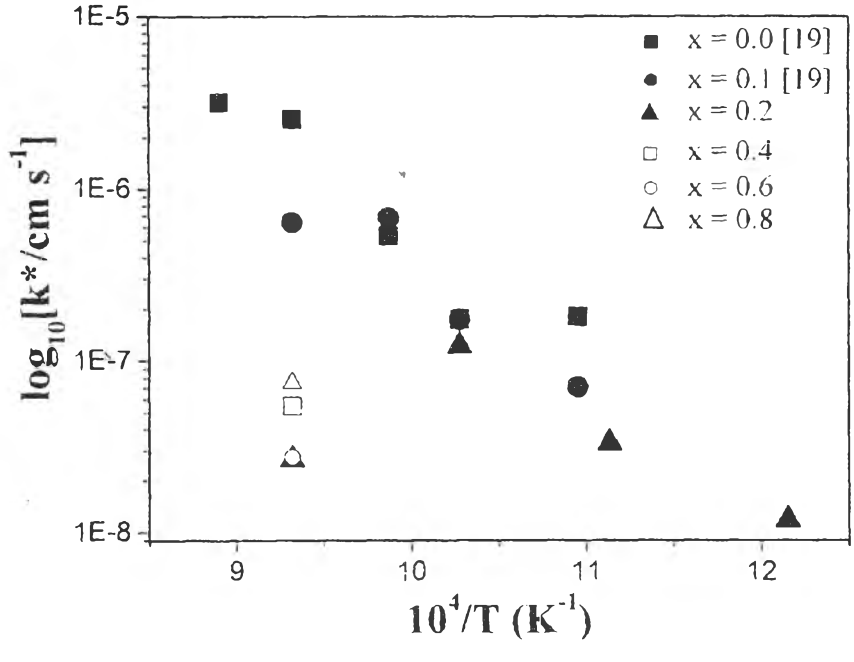

(b)

Figure 5.4 Arrhenius plot of (a) tracer diffusion coefficients (D*) and (b) surface exchange coefficient (k*) for of $La_{2-x}Sr_xNiO_{4+\delta}$.